34. BASALT WEATHERING ON THE EAST PACIFIC RISE AND THE GALAPAGOS SPREADING CENTER, DEEP SEA DRILLING PROJECT LEG 54

Susan E. Humphris,[1] Department of Geology, Imperial College of Science and Technology, Prince Consort Road, London SW7 2BP, England

William G. Melson, Department of Mineral Sciences, Smithsonian Institution, Washington, D.C.

and

Robert N. Thompson, Department of Geology, Imperial College of Science and Technology, Prince Consort Road, London SW7 2BP, England

ABSTRACT

The mineralogical and geochemical changes during the early stages of weathering of two suites of basalts from the East Pacific Rise and from the hydrothermal mound area near the Galapagos Spreading Center have been investigated. Three compositional groups of smectites were observed: an FeO^* and K_2O-rich variety, an MgO-rich type most closely resembling saponite, and a group with compositions intermediate between them. Other secondary minerals included carbonates, particularly an Mn-rich variety, hydrated iron oxides, and minor pyrite.

Geochemical comparison of the weathered rims and fresh interiors of individual samples indicated an increase in the K_2O and Rb contents and Fe_2O_3/FeO ratio, and a slight decrease in the CaO content in the weathered rims, even though their H_2O^+ contents were often less than 1 per cent.

The similar weathering processes that appear to have affected both suites of rocks, and the absence of any secondary minerals that are formed exclusively under hydrothermal conditions in the samples from the hydrothermal mounds area, would indicate that either circulation may be confined to a few narrow fractures — thereby restricting high-temperature alteration to the margins of basalts adjacent to the fractures — or that most of the hydrothermal minerals are formed at greater depths in the basaltic column.

INTRODUCTION

Interactions between sea water and rock at various temperatures in the oceanic crust have recently been studied in attempts to assess their importance for elemental fluxes into and out of the oceans (e.g., Thompson, 1973; Humphris and Thompson, 1978; Donnelly et al., in press; and Humphris et al., in press). Most of these studies have been confined to rocks dredged or drilled in the Atlantic Ocean. Although our knowledge of mineralogical and chemical variations during reactions with sea water is improving, our understanding of alteration processes as a function of age, basalt chemistry, and tectonic setting is very limited.

The purpose of this paper is to investigate the early stages of weathering (i.e., less than 3 m.y.B.P.) in two suites of samples recovered during Leg 54 which originated at different spreading centers in the Pacific Ocean — the East Pacific Rise and the Galapagos Spreading Center. The basalts erupted at these two spreading centers are chemically distinct from each other (Fodor et al., Srivistava et al., and Humphris et al.; all this volume) and from Mid-Atlantic Ridge basalts.

In addition, the samples studied also represent several different tectonic settings. Three major structural features were drilled in the region of the East Pacific Rise near 9°N (Figure 1): the East Pacific Rise flank fabric (Sites 420, 421, 423, and 429), the east–west trending OCP Ridge (Sites 422 and 428), and the Siqueiros fracture zone (Site 427). The Galapagos Spreading Center drilling included a north–south transect across a hydrothermal field 22 km south of the spreading center, which had previously been surveyed by Klitgord and Mudie (1974) and Lonsdale (1977) — Site 424. The basalts were overlain by hydrothermal sediments and so could have been subjected to a thermal regime different from that of the other sites. Site 425 was located 62 km north of the Galapagos Spreading Center in an area characterized by high heat flow.

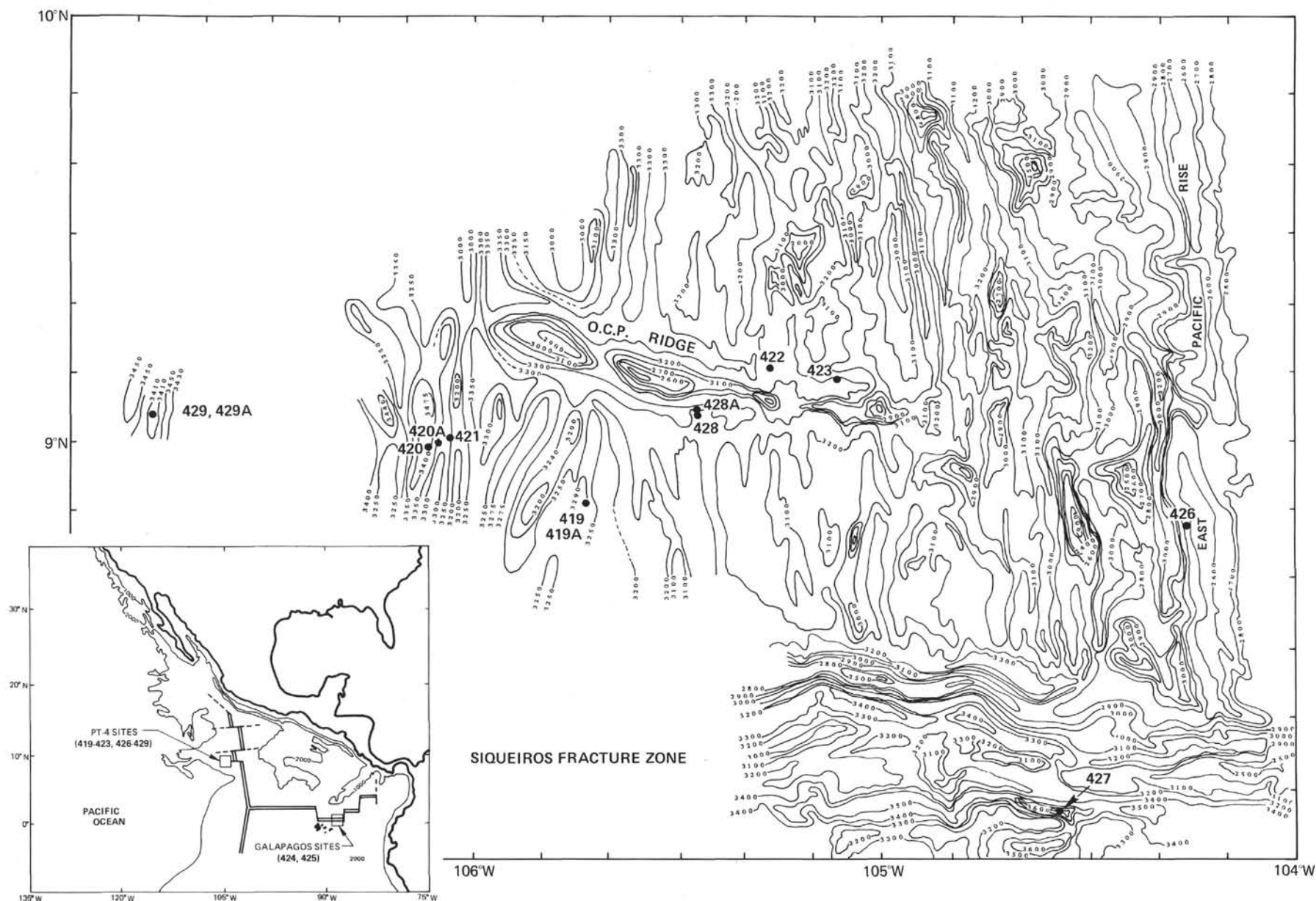[1] Present address: Sea Education Association, Woods Hole, Massachusetts.

Figure 1. *The location of sites drilled on Deep Sea Drilling Project Leg 64 near the East Pacific Rise and Galapagos Spreading Center (inset).*

ALTERATION MINERALOGY

Weathering processes affecting all the rocks recovered on Leg 54 have generally been confined to the infilling of veins and vesicles by clay minerals and carbonates, and to the formation of surface coatings on samples from both the East Pacific Rise and the Galapagos Spreading Center. In addition, many of the samples exhibit a well-defined rim, which is usually 1 to 3 cm wide and pale grey in color. Minor alteration of phenocrysts and groundmass phases and infilling of vesicles appear to have been responsible for this zonation. These weathered rims indicate that many of the rock surfaces have been exposed to sea water, suggesting that the oceanic crust in this area consists of highly jointed flows or small pillows.

Surface Coatings

Clay minerals constitute the most abundant surface coating and are found lining depressions in rock surfaces and infilling vugs in samples from the East Pacific Rise and the Galapagos Spreading Center. They are usually pale green or blue in color and form coatings of up to 1 mm thick. Scanning electron microphotographs indicate that these surface coatings are composed of a complex network of ramose (branching, twig-like) structures which project from the rock surface (Plate 1, Figure 1). Details of these ramose structures are shown in Plate 1 (Figure 2), which illustrates the radiating and interwoven nature of the clay mineral plates. Several samples of this surface coating were removed for X-ray diffraction study. Glycerol saturation of oriented samples results in expansion of the basal spacing from 14Å to 17.5Å, which subsequently collapsed on heating. A 060 peak of 1.533Å was observed, indicating that this smectite is trioctahedral.

The smectites are often associated with later-stage carbonates. Large vugs up to 1.2 cm in diameter (in Section 427-9-2, Piece 4) show two generations of calcite, and calcite veins are common in many samples. X-ray diffraction and qualitative analysis using an energy dispersive X-ray spectrometer (EDAX) were used to identify a manganese-rich calcite. The latter occurred as a cream, globular surface deposit found on samples from Hole 427 in the Siqueiros fracture zone (Plate 2, Figure 1). Scanning electron microphotographs (Plate 2, Figures 2 and 3) indicate that these globules are composed of parallel columns of stacked platelets. X-ray diffraction data are given in Table 1 and, although the major calcite peaks are clearly distinguishable, the whole pattern is slightly displaced owing to the manganese substitution. A manganese-rich carbonate has been observed replacing plagioclase phenocrysts in highly weathered basalts from the Bermuda Rise (Humphris et al., in press), but its existence as a surface deposit has thus far not been reported from ocean floor basalts.

Hydrated iron oxides cover the surface of many samples, and these are often associated with glassy margins of pillows or flows that are partially weathered. Pyrite occurs in small surface depressions (e.g., Section

TABLE 1
XRD Data for Manganese-Rich Calcite[a]

hkl	d Spacing (Å)	Intensity
104	2.958	Very strong
018	1.868	Strong
116	1.812	Medium (broad)
113	2.224	Medium
202	2.035	Weak
110	2.462	Very weak

[a]Section 427-9-2, Piece 5; Radiation FeK α.

427-11-1, Piece 3) or in vesicles (e.g., Section 425-9-3, Piece 5), but is extremely rare.

Basalt Alteration

It should be emphasized that all of the samples show only the early stages of weathering — i.e., infilling of some vesicles and veins, very occasional phenocryst alteration, and minor patchy replacement of the groundmass. Generally, less than 2 per cent of the rock has been affected, and this is confined to the outer weathered rim. Basalts from Site 425 near the Galapagos Spreading Center appear to be the most altered, with up to 4 volume per cent being affected. Samples with doleritic textures (i.e., from the OCP Ridge Sites 422 and 428, and from some sections of the Siqueiros fracture zone, Site 427) appear to have been less affected by weathering (less than 1 vol. %) than the quenched basalts. Alteration of phenocrysts is observed in only a few samples, and olivine appears to be the most affected phase. It is pseudomorphed by fine-grained aggregates of green smectite, which are often associated with hydrated iron oxides (eg., Section 427-11-1, Piece 4), or occasionally with cubes of pyrite (e.g., Section 428A-1-1, Piece 13). This smectite varies in color from bright green to yellow-green, and exhibits blue-green interference colors. In Hole 424C, drilled on the Galapagos Spreading Center, the olivine is replaced by a low birefringent, orange-brown smectite. In Section 429A-1-1, Piece 5, some plagioclase phenocrysts are replaced by white to pale green clay minerals with an infilling of calcite, but plagioclase alteration did not occur at any other site.

The groundmass of many basalts contains small patches of clay minerals. Bright green smectites are the most abundant, but light brown and orange-brown clay minerals do occur. The orange-brown smectites also form narrow rims outlining crystals. A relatively common feature is color zonation of the larger patches from green rims to light brown to red in the centers. The interiors are opaque and dark red, and resemble hydrated iron oxides. However, attempts to analyze these by microprobe indicate that they probably consist of intimate mixtures of iron oxides and clay minerals. Calcite occurs as a minor secondary mineral replacing the groundmass, particularly in samples from Sites 428 and 427, where it may or may not be associated with smectites.

Vesicles commonly contain secondary minerals in the weathered rims of the basalts, but are usually empty in the interiors. They are filled with: (1) bright green smectites; (2) light brown smectites; (3) a fine-scale zonation of green rims and brown interiors; (4) bright orange-brown smectites, similar in appearance to those rimming crystals; (5) dark red mixtures of hydrated iron oxides and smectites; (6) green or brown smectite lining with a core of chalcedony (Site 429A); and (7) in Section 425-7-1, Piece 6, a green rim infilled with white radiating needles of a zeolite. Different vesicle fillings occur within a single sample. However, the proportion of orange-brown and light brown smectites to green smectites appears to increase toward the margin of the samples. This may be related to the oxidation state of the iron in the smectite and not to a compositional change.

Representative microprobe analyses of the clay minerals from both the East Pacific Rise and the Galapagos Spreading Center are reported in Table 2; each result is the average of at least five analyses. For all sites, the major type of smectite is enriched in FeO* (expressing total Fe) and K_2O. This occurs as pseudomorphs after olivine, replacing the groundmass and infilling vesicles. Its color varies from bright green to light brown and its composition is generally characterized by low Al_2O_3, 26 to 30 per cent FeO*, 1 to 5 per cent MgO, and up to 6 per cent K_2O content. The bright orange-brown smectite that rims crystals and replaces the groundmass contains a higher concentration of iron — up to 36 per cent in Section 429A-1-1, Piece 5. Two other distinctly different compositions can be observed. The white to pale green smectite replacing the plagioclase phenocrysts appears to resemble saponite most closely in composition (Table 2, analyses 20 and 21), and contains 22 to 24 per cent MgO and 5 to 6 per cent FeO*. This mineral was identified only in Hole 429A, and only in this mineralogical setting.

The other compositional variation observed is intermediate between the Fe-rich and Mg-rich types, and this smectite occurs as a bright green vesicle filling in Sample Section 428A-3-1, Piece 11 (Table 2, Analysis 8). It contains 22 per cent FeO* and 14 per cent MgO, and may represent either a fine-grained mixture of two smectites or a mixed-layer clay mineral.

All the microprobe data from this study are plotted on a triangular SiO_2–FeO*–MgO diagram, with the weight percentages of K_2O plotted on a vertical axis (Figure 2). These are compared with clay mineral compositions from 110-m.y.-old basalts from the Bermuda Rise (Humphris et al., in press) and from 40-m.y.-old basalts from the Peru Trench (Scheidegger and Stakes, 1977). This comparison shows that Fe- and K-enriched smectites are the most abundant type of clay mineral found in the basalts studied from both the Atlantic and Pacific Oceans. However, the clay minerals found in the East Pacific Rise and Galapagos Spreading Center basalts are generally more Fe-rich than those from the Bermuda Rise. This could be related either to the higher FeO* content of the more evolved Pacific basalts, which may influence the composition of the fluid from which

the clay minerals formed, or to later cation exchange of the clay minerals from the Atlantic.

The "saponite-type" smectites replacing phenocrysts in Hole 429A are some of the most Mg-rich clay minerals analyzed from ocean floor basalts, and their formation is probably the result of rigidly localized physical and chemical conditions. A separate compositional group intermediate between the Mg-rich and Fe-rich end members is comprised of smectites from the Peru Trench and from the Bermuda Rise basalts. The absence of these intermediate smectites in the young East Pacific Rise and the Galapagos Spreading Center basalts suggests they are formed at a later stage of alteration, either by precipitation from a fluid of different composition or by cation exchange in pre-existing clay minerals.

GEOCHEMISTRY

Although all of the basalts recovered during Leg 54 are less than 5 m.y. old and appear relatively fresh, the early stages of alteration and formation of clay minerals should be reflected in changes in the bulk chemistry. Thirteen samples, for which the weathered rims previously discussed could be separated from the fresh cores, were selected for X-ray fluorescence (XRF) analyses. This approach permits direct comparison of the composition of the weathered rims with that of their fresh precursors; hence, it eliminates errors involved in assuming the composition of the fresh rock. Precision and accuracy of the analytical methods used are discussed in Humphris et al. (this volume). Details of the lithology, texture, and petrology of the selected samples are presented in Table 3.

Major- and selected trace-element analyses are presented in Table 4. Although most of the H_2O^+ contents are less than 1 per cent, with only three rims showing higher concentrations, it is clear that some of the oxides and elements, particularly Fe_2O_3, K_2O, and Rb, show significant alteration effects.

To make comparisons of the fresh interiors to the altered rims more meaningful, it is necessary to normalize the data. This can be accomplished by taking the ratio of each oxide to one that is relatively unaffected by weathering, such as alumina or titania. If the concentrations of both these oxides are unchanged by weathering, then their ratio in the fresh sample interior should be equal to that in the altered rim. This is illustrated in Figure 3, which demonstrates that the ratio of Al_2O_3/TiO_2 remains virtually unchanged during alteration of these samples. Thus, either Al_2O_3 or TiO_2 could be used for normalization; we will, however, use Al_2O_3 in this discussion since it is present in higher concentrations.

The most significant variations in chemical composition are observed in the iron concentrations. All the samples indicate that there is an increase in the total iron concentration during weathering (Figure 4), although this increase is not as pronounced in the more crystalline samples from the OCP Ridge and the Galapagos Spreading Center. Mineralogically, this is exhibited by the high iron content of the smectites replacing the groundmass and forming pseudomorphs after olivine. Oxidation has also been an important weathering pro-

cess — the Fe_2O_3 content of the rims is greater than that of the cores (Figure 5) — and the ferrous component shows only minor variations in concentrations (Figure 6). This would indicate that important changes in the concentrations of oxides occur during the earlier stages of weathering, which would not be evident from a bulk chemical analysis of a rock and its H_2O^+ content. Such variations, particularly in the iron concentration, may affect conclusions drawn from norm calculations and from magma fractionation modeling.

The slightly lower CaO contents of most of the altered rims in comparison with the fresh cores (Figure 7)

are in agreement with the decrease in calcium generally observed in more highly weathered basalts (e.g., Hart, 1970; and Thompson, 1973). Strontium also shows a decrease in concentrations in the weathered rims. The slightly higher CaO contents of the rim shown by two of the samples are probably a consequence of either minor replacement of the groundmass by calcite or of the incorporation of calcite veinlets into the sample.

The concentrations of MgO show some scatter about the line and, in general, appear to show only minor variations (Figure 8). However, higher MgO contents in the rims are indicated for a few samples. Since there is no

TABLE 2
Representative Microprobe Analyses of Clay Minerals from Basalts of the East Pacific Rise and the Galapagos Spreading Center

Wt. % Oxide	1[b]	2[c]	3[d]	4[e]	5[f]	6[g]	7[h]	8[i]	9[j]	10[k]	11[l]	12[m]	13[n]
SiO_2	49.70	47.46	47.20	47.91	48.45	48.37	50.84	47.25	49.89	47.46	51.04	48.57	53.62
Al_2O_3	6.17	3.44	4.61	4.14	3.30	0.07	0.22	3.04	0.32	3.12	4.72	4.32	0.43
$FeO*$[a]	26.14	27.75	27.70	26.93	28.13	31.91	28.20	22.47	28.37	31.64	28.35	29.15	22.61
MgO	2.91	3.04	2.97	3.08	3.15	3.36	4.74	14.20	4.53	1.83	1.83	2.08	6.54
CaO	0.24	0.09	0.18	0.22	0.16	0.84	0.64	1.51	0.72	0.30	0.79	0.26	0.31
K_2O	5.36	5.88	5.84	5.90	6.01	4.66	4.73	0.52	4.38	3.41	2.87	3.93	4.96
Na_2O	0.14	0.17	0.06	0.09	0.04	0.05	0.03	0.07	0.04	0.16	0.47	0.21	0.01
TiO_2	0.10	0.06	0.05	0.10	0.07	0.03	0.03	0.07	0.03	0.02	0.15	0.05	0.02
MnO	0.05	0.09	0.12	0.10	0.07	0.04	0.03	0.45	0.04	0.09	0.15	0.08	0.13
Total	90.83	87.97	88.73	88.46	89.39	89.32	89.46	89.58	88.31	88.04	90.36	88.65	88.63

Wt. % Oxide	14[o]	15[p]	16[q]	17[r]	18[s]	19[t]	20[u]	21[v]	22[w]	23[x]	24[y]	25[z]	26[aa]	27[bb]
SiO_2	49.97	49.89	49.22	42.58	43.29	40.10	50.44	50.95	52.60	53.63	51.20	52.65	51.54	52.03
Al_2O_3	0.97	0.65	0.59	1.04	0.45	0.77	3.62	3.26	3.77	2.99	3.82	4.70	0.42	0.36
$FeO*$[a]	30.24	28.74	30.03	34.29	35.58	35.51	6.19	5.70	26.94	27.49	28.50	28.93	24.28	27.87
MgO	3.72	3.99	3.57	7.89	5.38	9.42	22.83	23.60	2.39	2.36	1.48	1.56	5.45	4.20
CaO	0.37	0.28	0.40	0.53	0.29	0.46	0.25	0.20	0.52	0.40	0.50	0.83	0.37	0.40
K_2O	5.99	6.33	6.12	2.58	3.77	1.23	0.27	0.30	3.10	2.77	2.52	2.13	6.07	6.27
Na_2O	0.03	0.01	0.07	0.10	0.06	0.05	0.05	0.09	0.07	0.07	0.08	0.11	0.10	0.09
TiO_2	0.03	0.03	0.04	0.03	0.03	0.04	0.06	0.04	0.05	0.05	0.06	0.07	0.03	0.03
MnO	0.05	0.04	0.05	0.10	0.07	0.08	0.05	0.06	0.15	0.15	0.05	0.09	0.06	0.08
Total	91.37	89.97	90.10	89.15	88.91	87.66	83.77	84.22	89.60	89.91	88.22	91.05	88.32	91.33

[a]$FeO*$ = total iron expressed as FeO.
[b]Green clay mineral associated with hydrated iron oxide pseudomorphing olivine phenocryst: Section 427-11-1, Piece 4;
[c]Green clay mineral replacing groundmass: Section 427-11-1, Piece 4;
[d]Green clay mineral pseudomorphing olivine: Section 427-11-1, Piece 4;
[e]Green clay mineral after olivine: Section 427-11-1, Piece 4;
[f]Yellow-green vein filling: Section 427-11-1, Piece 4;
[g]Green clay mineral replacing groundmass: Section 428A-3-1, Piece 11;
[h]Green clay mineral replacing groundmass: Section 428A-3-1, Piece 11;
[i]Green smectite infilling vesicle: Section 428A-3-1, Piece 11;
[j]Green smectite replacing groundmass: Section 428A-3-1, Piece 11;
[k]Orange-brown smectite replacing groundmass: Section 424C-2-1, Piece 4;
[l]Orange-brown smectite pseudomorphing phenocryst: Section 424C-2-1, Piece 4;
[m]Orange-brown clay mineral replacing groundmass: Section 424C-2-1, Piece 4;
[n]Interior of vesicle: Section 429A-1-1, Piece 5;
[o]Outer rim of same vesicle: Section 429A-1-1, Piece 5;
[p]Green smectite infilling small vesicle: Section 429A-1-1, Piece 5;
[q]Green vesicle filling: Section 429A-1-1, Piece 5;
[r]Orange-brown clay mineral replacing groundmass: Section 429A-1-1, Piece 5;
[s]Brown clay mineral replacing groundmass: Section 429A-1-1, Piece 5;
[t]Brown clay mineral replacing groundmass: Section 429A-1-1, Piece 5;
[u]White-pale green smectite replacing plagioclase phenocryst and associated with calcite: Section 429A-1-1, Piece 5;
[v]Pale green smectite replacing plagioclase phenocryst: Section 429A-1-1, Piece 5;
[w]Green smectite infilling vesicle: Section 421-3-1, Piece 20;
[x]Green vesicle filling: Section 421-3-1, Piece 20;
[y]Green smectite replacing groundmass: Section 421-3-1, Piece 20;
[z]Green smectite replacing groundmass: 54-421-3-1-20;
[aa]Green rim of vesicle infilled with zeolite: Section 425-7-1, Piece 6; and
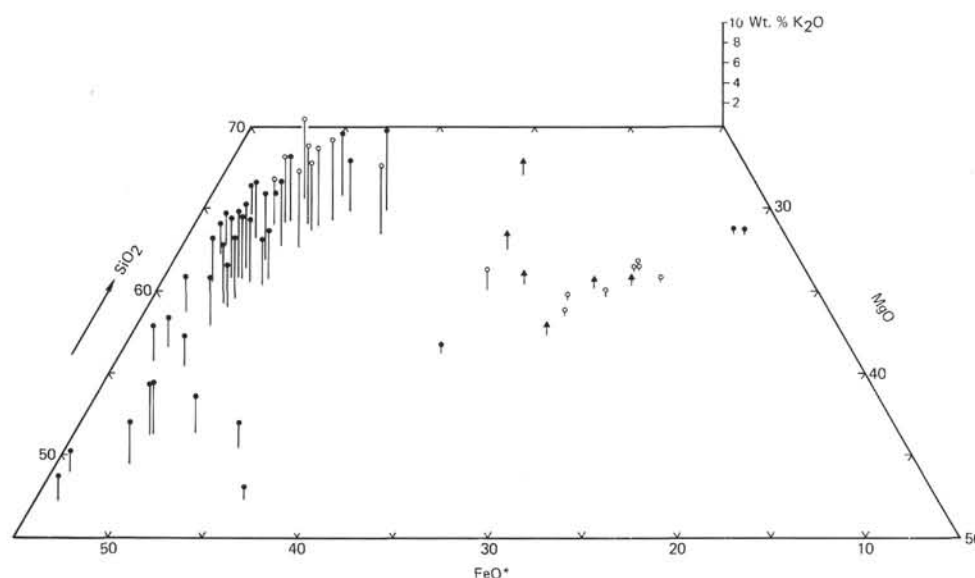[bb]Green vesicle filling: Section 425-7-1, Piece 6.

Figure 2. SiO_2–FeO^*–MgO triangular diagram, with wt. % K_2O plotted on a vertical axis, presenting the composition of secondary clay minerals found in some weathered oceanic basalts (FeO expresses total Fe). = clay minerals from the East Pacific Rise and Galapagos Spreading Center (this study); = clay minerals from the Bermuda Rise, Atlantic Ocean (Humphris et al., in press); = clay minerals from the Peru Trench (Scheidegger and Stakes, 1977).

evidence for uptake of significant quantities of MgO in the compositions of the smectites from these samples, these variations in the MgO content may be a reflection of inhomogeneous distribution of primary phases within the thin flows or pillows.

Previous studies have shown that K_2O is generally taken up during basalt weathering, and it has been suggested that this process may be an important sink for potassium in the oceans (e.g., Melson and Thompson, 1973; Donnelly et al., in press; and Humphris et al., in press). The weathered rims of the young basalts from the East Pacific Rise and the Galapagos Spreading Center also show overall increases in the K_2O content of the rocks (Figure 9) with concomitant increases in the Rb concentrations. This is the result of formation of the K- and Fe-enriched smectites in these samples. The K_2O concentrations observed in the fresh interiors of the more crystalline samples are lower than those found in the finer grained basalt. This may indicate that weathering has affected the interiors of the fine-grained basalts as well as the rims, whereas the crystalline cores have retained a K_2O content closer to their original levels. Ocean floor basalts clearly provide a sink for K and begin to remove this element from sea water during the very early stages of weathering. These results suggest that the bulk rock K_2O content is affected by the initial weathering processes which consist mostly of clay mineral formation in vesicles, and which may affect only 1 per cent of the rock. Many of the basalts dredged or drilled from the ocean floor contain smectite-filled vesicles, suggesting that the early stages of weathering are a common feature. These observations would therefore support the contention that weathering can be an important sink for potassium in the oceans.

Variations in Na_2O concentrations are small and show no consistent trends, suggesting that the early stages of weathering do not alter the Na_2O contents of the basalts (Figure 10). This is in contrast with studies of more highly weathered basalts, in which uptake of Na_2O has been observed (Hart, 1970).

DISCUSSION AND CONCLUSIONS

The major type of alteration in the basalts from Leg 54 is the formation of smectites. There is no evidence for their absolute temperature of formation, but the lack of zeolites and chlorite suggests that alteration occurred predominantly at low temperatures. Smectite formation, the presence of calcite, and the increase in the Fe_2O_3/FeO ratio in the weathered rims indicate that alkaline, oxidizing conditions (which could be provided by sea water) prevailed during alteration of these rocks. The occurrence of chemically similar smectites from the East Pacific Rise, the Galapagos Spreading Center, and the Bermuda Rise suggests that K- and Fe-enriched smectites can be formed regardless of variations in basalt chemistry. If these smectites are typical of the early stages of low-temperature weathering of basalts, this would indicate that the chemical variations in the composition of the basalts are initially unimportant. This may be explained by the observation that olivine and the interstitial material are usually the first to be altered. It is not until other phases, such as plagioclase and pyroxene, are altered, that the effects of variations in basalt chemistry are detected. For instance, the smectites from these young basalts contain very little alumina. However, it is likely that as weathering advances, and plagioclase is altered, the smectites formed will be more aluminous.

TABLE 3
Samples Subjected to Bulk Chemical Analyses of their Fresh Interiors and Weathered Rims

Specimen	Location	Lithology	Texture	Petrographic Notes	
				Fresh Interior	Weathered Rim
Section 420-14-1, Piece 3	EPR flank fabric	Interior of highly jointed flow	Aphyric; fine-grained	Plagioclase, clinopyroxene, minor olivine, glass	Green smectite patchily replacing groundmass. Zoned vesicles. Weathering − 2%
Section 421-3-1, Piece 14	EPR flank fabric	Fragment of highly jointed thin flow	Fine-grained; isolated pcs with glomerophyric clusters	Plagioclase and olivine phyric	Green and brown smectites replacing groundmass and filling vesicles. Weathering < 1%
Section 421-3-1, Piece 18	EPR flank fabric	Fragment of highly jointed thin flow	Fine-grained; glomerophyric	Plagioclase and olivine glomerocrysts. Empty vesicles	Patchy replacement of groundmass. Filled vesicles. Weathering < 1%
Section 421-4-1, Piece 5	EPR flank fabric	Fragments of jointed flow or pillow	Glomerophyric	Plagioclase, olivine and clinopyroxene. Some vesicles filled	Patchy groundmass alteration. Vesicles filled with green smectites or zoned. Weathering − 1%
Sample 423-5-CC-1	EPR flank fabric	Edge of thin, basaltic flow	Fine-grained; variolitic	Plagioclase, clinopyroxene; dominantly glassy matrix	Green and orange-brown smectites fill vesicles and replace groundmass. Sulfides. Weathering ∼ 2%
Section 425-7-1, Piece 6	62 km north of Galapagos Spreading Center	Interior of cooling unit	Intersertal	Plagioclase, clinopyroxene, with minor glass. Vesicles empty	Green and brown smectites. Sulfide mineralization. Weathering − 1%
Section 425-9-3, Piece 5	62 km north of Galapagos Rift	Interior of cooling unit	Holocrystalline, equigranular	Plagioclase, clinopyroxene and opaques	Green clay minerals replacing groundmass. Weathering ∼ 1%
Section 428A-2-1, Piece 2	South side of OCP Ridge	Interior of thin flow	Cryptocrystalline, massive	Plagioclase, clinopyroxene and minor olivine	Groundmass patchily replaced by smectites, sometimes with sulfide. Weathering < 1%
Section 428A-6-1, Piece 6	South side of OCP Ridge	Interior of slowly cooled unit	Equigranular	Plagioclase, clinopyroxene and opaques	Patchy groundmass replacement by brown smectites. Weathering ∼ 1%
Section 428A-6-1, Piece 14	South side of OCP Ridge	Interior of slowly cooled unit	Equigranular	Plagioclase, clinopyroxene and opaques	Green-brown smectites replacing groundmass. Weathering ∼ 1%
Section 429A-2-1, Piece 8	EPR flank fabric	Pillow basalt or highly fractured thin flow	Fine-grained; variolitic to intersertal	Plagioclase phyric with plagioclase, clinopyroxene and opaques	Green smectites replacing groundmass and infilling vesicles. Weathering < 1%
Section 429A-2-1, Piece 10	EPR flank fabric	Pillow basalt or highly fractured thin flow	Fine-grained; variolitic to intersertal	Plagioclase phyric	Green smectites replacing groundmass and infilling vesicles. Weathering < 1%
Section 429A-2-1, Piece 16	EPR flank fabric	Pillow basalt or highly fractured thin flow	Fine-grained; variolitic to intersertal	Plagioclase phyric with plagioclase, clinopyroxene and glass	Green smectites replacing groundmass and infilling vesicles. Weathering ∼ 1%

The lack of any secondary minerals formed exclusively under hydrothermal conditions at Site 424 in the hydrothermal mounds area near the Galapagos Spreading Center has important implications for circulation of fluids through the oceanic crust. Although overlain by hydrothermal sediment deposits, the samples recovered show only traces of weathering, resembling those at all other sites. There are two possible explanations for this observation. The first is that even in highly jointed flows such as those that constitute the crust in this region, circulation may be confined to a few narrow fractures, thereby restricting reactions to a thin margin of

TABLE 4
Core and Rim Chemical Analyses for Individual Samples Recovered During Leg 54

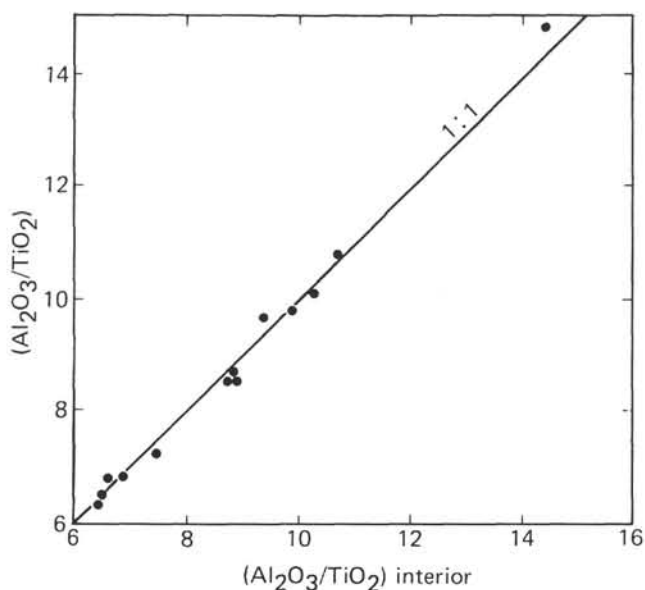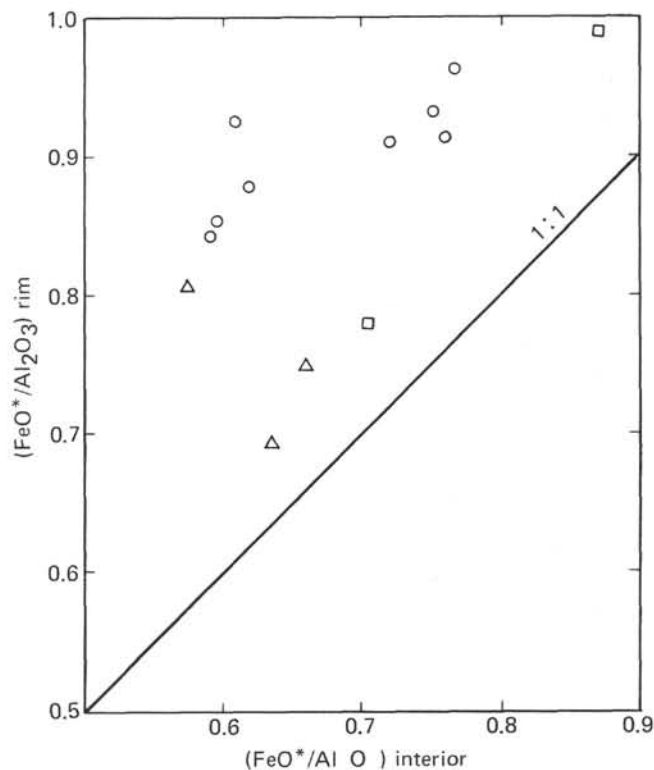| Specimen:	423-5-CC, Piece 1		428A-2-1, Piece 2		428A-6-1, Piece 6		428A-6-1, Piece 14		421-3-1, Piece 14		421-3-1, Piece 18	
	Outer Rim	Core	Outer Rim	Core	Outer Rim	Core	Outer Rim	Core	Outer Rim	Core	Outer Rim	Core
SiO_2[a]	50.81	51.18	50.80	51.56	49.74	50.63	50.70	50.52	50.41	51.55	49.88	51.02
Al_2O_3	13.99	14.43	14.65	15.71	15.07	15.47	14.99	15.23	14.00	14.63	13.83	14.54
Fe_2O_3	4.82	2.07	5.63	3.15	4.17	2.61	4.99	3.32	5.38	3.42	5.36	3.83
FeO	7.18	8.01	5.41	5.27	5.66	6.53	5.57	6.06	6.67	6.38	6.78	6.42
MgO	6.72	6.84	6.99	6.85	7.73	7.67	7.24	7.38	6.46	6.64	6.38	6.54
CaO	10.52	11.05	11.51	12.38	11.70	12.22	11.96	12.51	10.73	11.58	10.73	11.40
Na_2O	2.94	3.09	2.86	3.30	2.88	2.87	2.95	2.94	2.82	3.01	2.89	3.00
K_2O	0.48	0.31	0.50	0.22	0.27	0.15	0.43	0.16	0.52	0.35	0.57	0.34
TiO_2	2.05	2.14	1.51	1.58	1.38	1.45	1.47	1.48	2.06	2.24	2.12	2.25
P_2O_5	0.23	0.22	0.16	0.16	0.16	0.14	0.15	0.15	0.21	0.22	0.19	0.23
MnO	0.20	0.21	0.16	0.16	0.16	0.16	0.17	0.16	0.20	0.21	0.20	0.20
H_2O^+	0.82	0.59	0.65	0.30	0.61	0.67	0.87	0.55	0.91	0.67	1.02	0.41
CO_2	0.07	0.01	0.01	0.09	0.09	0.15	0.12	0.27	0.07	0.09	0.21	0.49
Total	100.83	100.15	100.88	100.73	99.62	100.74	101.61	100.73	100.44	100.99	100.16	100.67
Rb[b]	–	–	9	–	5	–	10	1	8	1	–	–
Sr	–	–	122	–	127	–	121	127	112	135	–	–
Y	–	–	25	–	25	–	27	29	42	48	–	–
Zr	–	–	96	–	90	–	95	93	132	141	–	–
Nb	–	–	4	–	4	–	4	4	6	7	–	–

Figure 3. Al_2O_3/TiO_2 ratios for the weathered rims and fresh interiors of basalts from the East Pacific Rise and the Galapagos Spreading Center. The solid line represents equal ratios in the rim and interior.

basalt adjacent to those fractures. This would indicate that hydrothermal alteration affects only a very small percentage of the oceanic crust, while low-temperature reactions affect a much larger volume of basalt.

The second explanation is that most of the hydrothermal minerals are formed at greater depths in the basalt column, and so were not recovered during drilling.
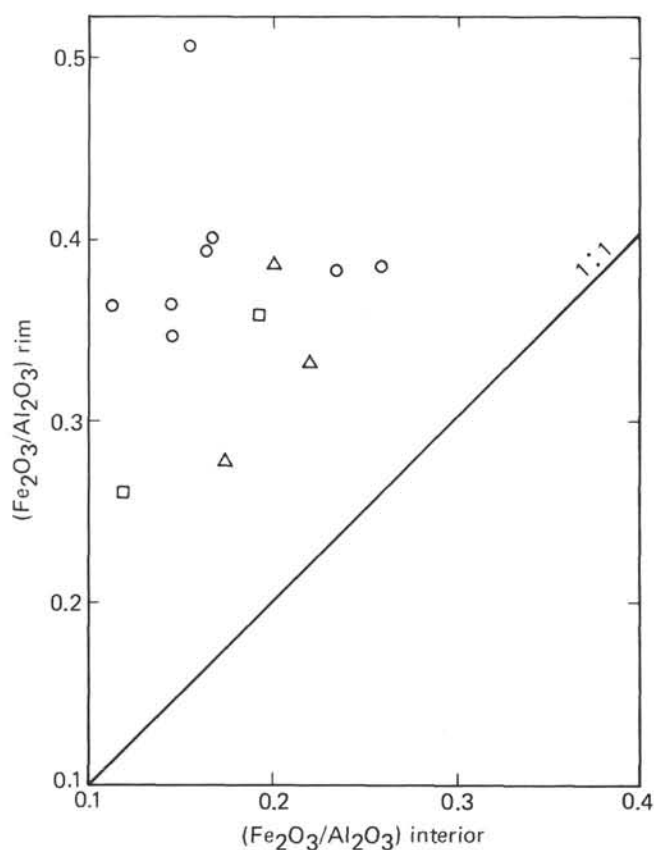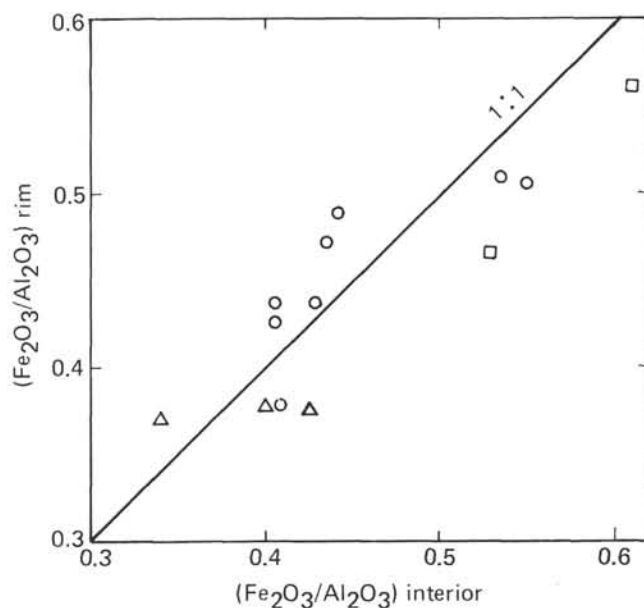

o = East Pacific Rise basalts
△ = OCP Ridge basalts
□ = Galapagos Spreading Center basalts

Figure 4. FeO^*/Al_2O_3 ratios in altered rims and fresh interiors, where FeO^* expresses total Fe.

TABLE 4 – *Continued*

421-4-1, Piece 5		420-14-1, Piece 3		429A-2-1, Piece 8		429A-2-1, Piece 10		429A-2-1, Piece 16		425-7-1, Piece 6		425-9-3, Piece 5	
Outer Rim	Core	Outer Rim	Core	Outer Rim	Core	Outer Rim	Core	Outer Rim	Core	Outer Rim	Core	Outer Rim	Core
50.54	50.93	50.84	52.14	50.30	52.16	50.59	52.32	50.51	51.65	51.57	51.82	50.85	51.53
13.68	14.42	14.20	15.07	14.21	15.03	14.19	15.05	14.19	15.02	13.63	14.18	14.61	14.73
5.37	2.36	7.18	2.29	5.01	1.65	5.14	2.17	5.72	2.53	4.89	2.69	3.77	1.67
7.05	7.85	5.38	6.20	6.28	6.48	6.28	6.13	6.10	6.10	7.72	8.73	6.86	7.81
6.22	6.12	5.83	6.40	6.85	7.00	6.87	7.00	6.86	7.05	6.95	7.39	7.85	8.16
10.64	10.83	10.78	11.56	11.36	11.64	11.20	11.95	11.08	11.86	10.81	11.50	12.01	12.51
2.87	3.05	2.85	3.00	2.80	3.09	2.87	3.16	2.92	3.01	2.45	2.39	2.18	2.26
0.48	0.36	0.67	0.31	0.50	0.23	0.51	0.31	0.50	0.27	0.43	0.05	0.34	0.07
2.18	2.27	1.96	2.04	1.65	1.71	1.64	1.70	1.66	1.70	1.39	1.43	0.98	1.02
0.20	0.20	0.19	0.17	0.15	0.19	0.16	0.17	0.21	0.18	0.18	0.13	0.11	0.10
0.21	0.16	0.17	0.20	0.18	0.19	0.19	0.19	0.18	0.19	0.19	0.20	0.17	0.19
0.67	0.51	1.45	0.47	0.69	0.77	0.89	0.69	1.27	0.60	0.60	0.34	0.80	0.53
0.11	0.09	0.06	0.08	0.07	0.05	0.11	0.04	0.05	0.04	0.01	0.13	0.06	0.12
100.22	99.15	101.56	99.93	100.05	100.79	100.64	100.88	101.25	100.20	100.82	100.98	100.59	100.70
4	0	–	0	9	–	–	–	–	–	8	1	–	2
108	136	–	135	111	–	–	–	–	–	54	57	–	55
46	49	–	42	30	–	–	–	–	–	32	35	–	24
142	146	–	134	103	–	–	–	–	–	74	77	–	43
6	4	–	5	6	–	–	–	–	–	4	1	–	2

[a]Oxide concentrations in wt. %.
[b]Concentrations in ppm.

Figure 5. *Fe_2O_3/Al_2O_3 ratios for weathered basalts of the East Pacific Rise and the Galapagos Spreading Center.*

Figure 6. *FeO/Al_2O_3 ratios in altered rims and fresh basalt interiors.*

Although hot hydrothermal fluids could percolate upward through the basalt, the highly fractured surface layers permit considerable mixing and dilution of these fluids by sea water, although some of the fluids must reach the sea floor to deposit the hydrothermal sediments. Hence, most of the evidence for hydrothermal circulation will be masked in the surface crustal layers by low-temperature rock–water interactions.
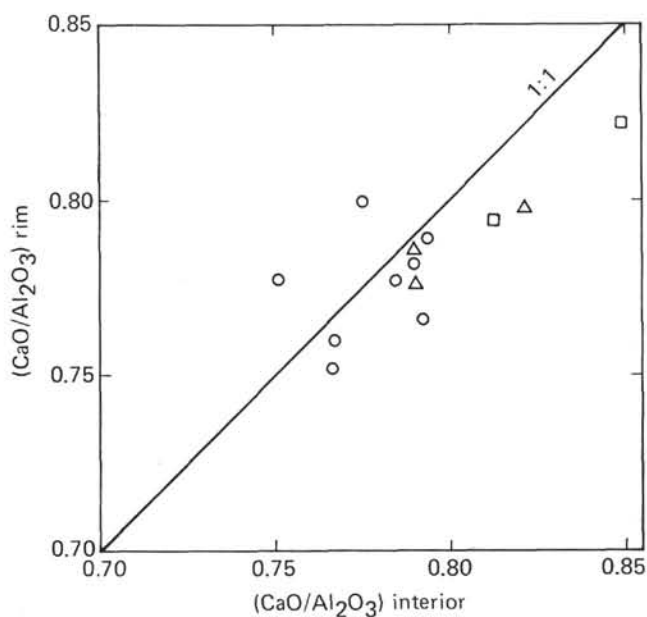
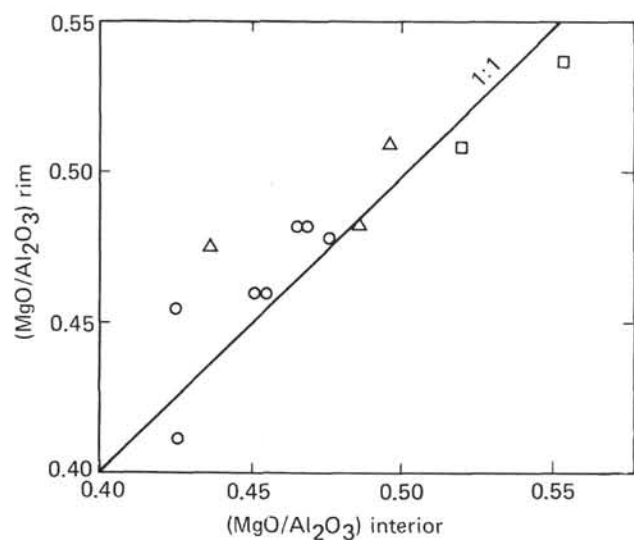Figure 7. *CaO/Al$_2$O$_3$ ratios in basalts displaying weathered rims.*

Figure 8. *MgO/Al$_2$O$_3$ ratios in basalts from the East Pacific Rise and the Galapagos Spreading Center.*

One of the most remarkable features of the alteration mineralogy and associated chemical variations is the similarity between all the sites, even though they represent different thermal and tectonic settings. This suggests there is an initial set of reactions that ocean floor basalts undergo after eruption, regardless of the prevailing environmental conditions. If this is the case, the K-and Fe-enriched smectites represent the initial response of the cooling basalt to reaction with sea water. These early alteration processes must therefore occur very shortly after the emplacement of the basalts on the sea floor.

Figure 9. *K$_2$O/Al$_2$O$_3$ ratios in basalts, showing uptake of K$_2$O during the early stages of weathering.*
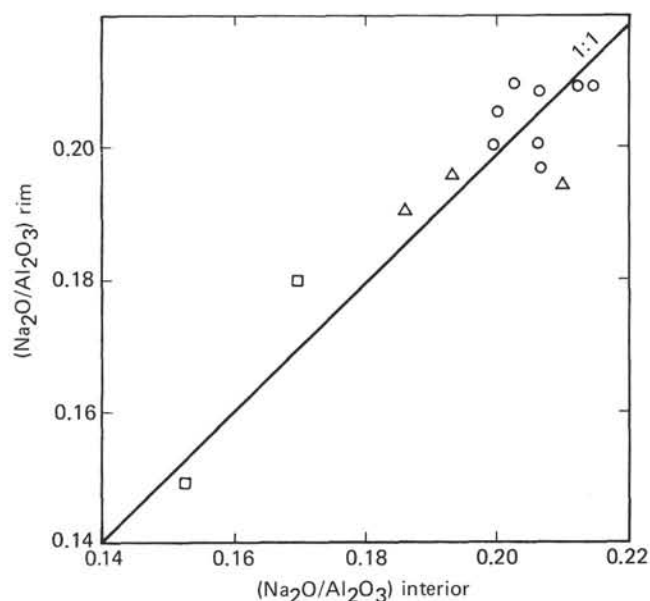

Figure 10. *Na$_2$O/Al$_2$O$_3$ ratios in weathered basalts from the East Pacific Rise and the Galapagos Spreading Center.*

REFERENCES

Donnelly, T., Thompson, G., and Salisbury, M. H., in press. The chemistry of altered basalts at Site 417, Deep Sea Drilling Project Leg 51. *In* Donnelly, T., Francheteau, J., Bryan, W., Robinson, P., Flower, M., Salisbury, M., et al., *Initial Reports of the Deep Sea Drilling Project,* v. 51, 52, 53, Part 2: Washington (U.S. Government Printing Office).

Hart, R., 1970. Chemical exchange between seawater and deep ocean basalts. *Earth Planet. Sci. Letts.,* v. 9, p. 269.

Humphris, S. E. and Thompson, G., 1978. Hydrothermal alteration of oceanic basalts by seawater. *Geochim. Cosmochim. Act,* v. 42, p. 1017.

Humphris, S. E., Thompson, R. N., and Marriner, G. F., in press. The mineralogy and geochemistry of basalt weathering, Holes 417A and 418A. *In* Donnelly, T., Francheteau, J., Bryan, W., Robinson, P., Flower, M., Salisbury, M., et al., *Initial Reports of the Deep Sea Drilling Project,* v. 51, 52, 53, Part 2: Washington (U.S. Government Printing Office).

Klitgord, K. D. and Mudie, J. D., 1974. The Galapagos Spreading Centre: a near bottom geophysical survey. *Geophys. J. Roy. Astr. Soc.,* v. 38, p. 563.

Lonsdale, P., 1977. Deep-tow observations at the mounds abyssal hydrothermal field, Galapagos Rift. *Earth Planet. Sci. Letts.,* v. 36, p. 92.

Melson, W. G. and Thompson, G., 1973. Glassy abyssal basalts, Atlantic sea floor near St. Paul's rocks: petrography and composition of secondary clay minerals. *Bull. Geol. Soc. Amer.,* v. 84, p. 703.

Scheidegger, K. F. and Stakes, D. S., 1977. Mineralogy, chemistry and crystallisation sequence of clay minerals in altered tholeiitic basalts from the Peru Trench. *Earth Planet. Sci. Letts.,* v. 36, p. 413.

Thompson, G., 1973. A geochemical study of the low temperature interaction of seawater and oceanic igneous rock. *Trans. Am. Geophys. Un.,* v. 54, p. 1015.
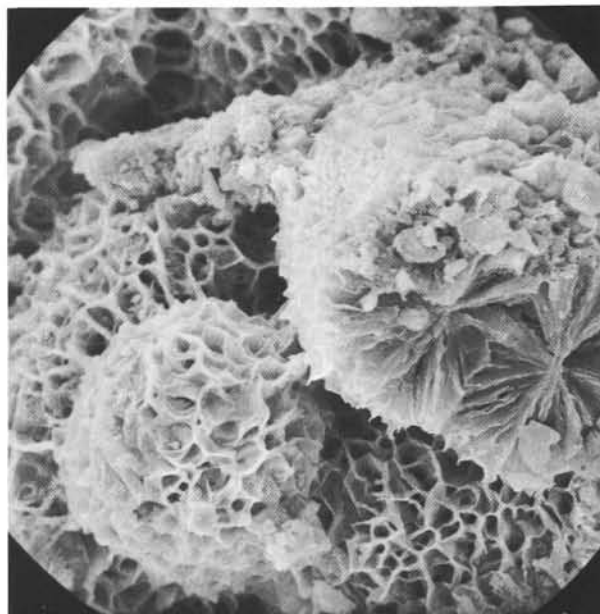
PLATE 1
Section 427-9-2, Piece 9A

Figure 1   Pale blue clay mineral composed of a complex net-
work of branching structures lining a vug.
Magnification: ×300

Figure 2   Detail of the branching structures illustrating the
radiating and interwoven nature of the clay miner-
al plates.
Magnification: ×1500

PLATE 1

1

2

PLATE 2
Section 427-9-2, Piece 12

Figure 1   Cream, globular deposit of manganese-rich calcite
            on rock surface.

Figure 2   Detail of surface deposit exhibiting parallel col-
            umns of stacked platelets.
            Magnification: ×860

Figure 3   Finer detail of manganese-rich calcite.
            Magnification: ×2400

PLATE 2

1

0   1cms

2

3